

Design of Next-Generation DGAT2 Inhibitor PF-07202954 with Longer Predicted Half-Life

Kevin J. Filipinski,* David J. Edmonds, Michelle R. Garnsey, Daniel J. Smaltz, Karen Coffman, Kentaro Futatsugi, Jack Lee, Steven V. O'Neil, Ann Wright, Deane Nason, James R. Gosset, Christine C. Orozco, Dan Blackler, Guila Fakhoury, Jemy A. Gutierrez, Sylvie Perez, Trenton Ross, Ingrid Stock, Gregory Tesz, and Robert Dullea



Cite This: *ACS Med. Chem. Lett.* 2023, 14, 1427–1433



Read Online

ACCESS |



Metrics & More



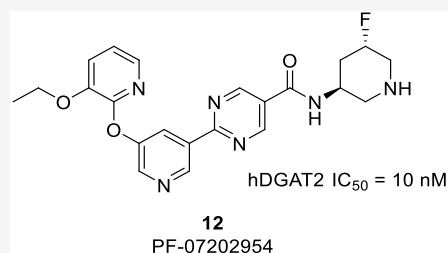
Article Recommendations



Supporting Information

ABSTRACT: Diacylglycerol O-acyltransferase 2 (DGAT2) inhibitors have been shown to lower liver triglyceride content and are being explored clinically as a treatment for non-alcoholic steatohepatitis (NASH). This work details efforts to find an extended-half-life DGAT2 inhibitor. A basic moiety was added to a known inhibitor template, and the basicity and lipophilicity were fine-tuned by the addition of electrophilic fluorines. A weakly basic profile was required to find an appropriate balance of potency, clearance, and permeability. This work culminated in the discovery of PF-07202954 (**12**), a weakly basic DGAT2 inhibitor that has advanced to clinical studies. This molecule displays a higher volume of distribution and longer half-life in preclinical species, in keeping with its physicochemical profile, and lowers liver triglyceride content in a Western-diet-fed rat model.

KEYWORDS: DGAT2, Diacylglycerol O-acyltransferase 2, NAFLD, NASH, Half-life, pK_a , Fluorination



Non-alcoholic fatty liver disease (NAFLD) is considered to be the most common liver disease in Western countries and is characterized by an excess of triglycerides in the liver.^{1,2} Non-alcoholic steatohepatitis (NASH) is a more severe form of NAFLD, which also includes inflammatory-driven liver injury and often fibrosis. In the liver, two enzymes catalyze the majority of triglyceride synthesis from fatty acyl-CoA and diacylglycerol, termed diacylglycerol O-acyltransferase 1 and 2 (DGAT1 and DGAT2).³ While these two enzymes share identical catalytic functions, they differ in tissue distribution, with DGAT1 being highly expressed in the small and large intestines. In clinical studies, DGAT1 inhibition impaired lipid absorption, leading to diarrhea and gastrointestinal discomfort. DGAT2, which is enriched in hepatocytes, has minimal intestinal expression, and thus, clinical inhibition of DGAT2 has not caused the gastrointestinal side effects observed with DGAT1 inhibition.⁴ Furthermore, these two acyl transferases utilize different lipid sources: DGAT2 prefers de novo-synthesized fatty acids, while DGAT1 prefers fatty acids derived from diet and lipolysis.³ It is hypothesized that by inhibiting DGAT2, liver fat content can be reduced and the progression of NASH can be slowed.^{5–7} There are currently no approved therapies for NASH, although several mechanisms are in advanced clinical development.⁸ DGAT2 inhibitors have been previously described (Figure 1)^{9–15} and shown to reduce hepatic steatosis in human subjects.¹⁶ At least one small-molecule DGAT2 inhibitor, ervogastat (PF-06865571),¹⁷ is currently in clinical studies, as

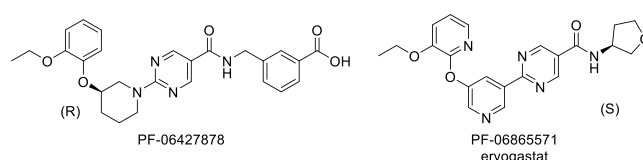


Figure 1. Structures of clinical candidate DGAT2 inhibitors.

well as LG203003.¹⁸ In addition, an antisense therapy, ION224, designed to decrease levels of DGAT2 protein, is under clinical investigation for NASH.^{19,20}

The goal of this discovery effort was to find a DGAT2 inhibitor with a longer predicted human half-life ($t_{1/2}$) as a backup to the clinical candidate ervogastat, which showed a human half-life of approximately 1.5–5 h in the single ascending dose phase 1 study.⁴ Extending half-life can have certain advantages in some cases, such as reducing the daily tablet burden, improving patient compliance, and reducing the peak-to-trough ratio.^{21,22} This last attribute may have

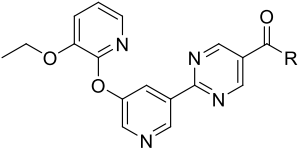
Received: July 27, 2023

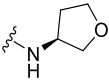
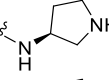
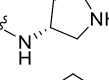
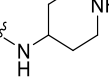
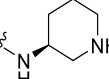
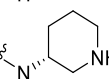
Accepted: September 26, 2023

Published: October 2, 2023



Table 1. SAR of Strongly Basic Amines



compound	R	hDGAT2 IC ₅₀ (nM) ^a	pK _a ^b	logD ^c	HHEP CL _{int,app} (μL/min/million) ^d	P _{app} (10 ⁻⁶ cm/sec) ^e
ervogastat		17 (5.1 – 59)	-	1.9	3.9 ^f	19
1		500 (240 – 1,000)	9.2	-0.19	<1.8	0.39
2		410 (110 – 1,600)	9.2	-0.15	<3.0	0.68
3		22,000 ^g	10.1	-0.19	NT ^h	1.3
4		3,100 (1,800 – 5,400)	9.5	0.35	<1.8	1.3
5		21,000 ^g	NT	0.3	NT	1.3

^aIC₅₀ values are reported as the geometric mean of $n \geq 3$ with the 95% confidence interval (CI) in parentheses, except where otherwise noted. ^bExperimental pK_a. ^clogD measured with the shake-flask method.³⁴ ^dApparent intrinsic clearance (CL_{int,app}) obtained from human hepatocyte cells.³⁵ ^ePermeability determined from an assay using low-efflux MDCKII cells.³⁶ ^fCL_{int,app} obtained from human hepatocyte cells using the relay method for low-clearance compounds.³⁷ ^g $n = 2$. ^hNT = not tested.

advantages when considering selectivity over off-targets, safety margins, and the drug–drug interaction potential.

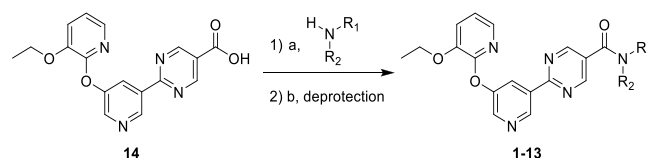
Our work to extend the predicted half-life began with the clinical DGAT2 inhibitor ervogastat. This is a neutral molecule, which accordingly has a moderate volume of distribution in preclinical species ($V_{ss} = 0.71$ and 0.91 L/kg in rat and monkey, respectively). Our approach to extending the half-life within this chemotype was to increase the volume of distribution by adding a basic center.²³ Basic compounds generally have higher volumes of distribution than acidic or neutral species, and this is hypothesized to occur due to their low affinity for plasma albumin and their electrostatic attraction to negatively charged phospholipid membranes.²¹ Since the half-life is directly proportional to the steady-state volume of distribution (V_{ss}) according to eq 1,

$$t_{1/2} = \ln(2) V_{ss} / CL \quad (1)$$

this can be a successful strategy if a basic center is tolerated in the target binding site and clearance (CL) is controlled. Bases can also show greater solubility compared to neutrals. Other strategies to increase half-life by focusing on reducing clearance (eliminating soft spots, deuteration, and increasing LipMetE) were pursued but did not result in success.

Based on the previous structure–activity relationship (SAR) explorations during the discovery of ervogastat, the amide vector offered the most productive optimization options. Hence, the initial effort to install a basic center on this scaffold was focused on the amide vector (Table 1). All analogues were synthesized according to the methods shown in Scheme 1 and

Scheme 1. Synthesis of Analogues 1–13^a

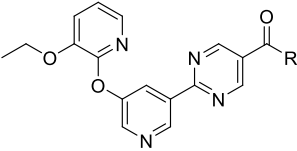


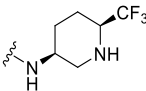
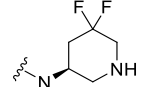
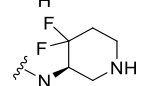
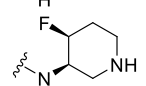
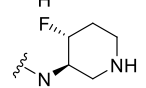
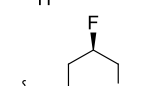
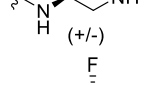
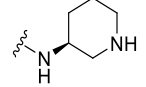
^a(a) Amidation conditions include HATU, DMC, or T3P; (b) where needed, Cbz deprotection using HCl or Boc deprotection using TFA.

the Supporting Information.²⁴ As in previous publications, a biochemical assay using human DGAT2 was used as the primary driver to explore potency. Compounds 1–5 include several unsubstituted pyrrolidine and piperidine amides. While these analogues were less potent, they did confirm that a basic nitrogen was somewhat tolerated, and the large decrease in logD compared to that of ervogastat may be partly responsible for the loss of potency. Each of these pyrrolidines and piperidines have pK_a > 9 and, as expected, displayed poor passive permeability. Consistent with its basicity and as shown in Table 3, 2 did have a higher volume of distribution and longer half-life in rat compared to ervogastat (2, $V_{ss} = 4.1$ L/kg and $t_{1/2} = 1.9$ h; ervogastat, $V_{ss} = 0.91$ L/kg and $t_{1/2} = 0.3$ h) when dosed intravenously.

Measurable potency and the proof of concept that increased volume of distribution leads to increased half-life were encouraging first steps. Further efforts to alter pK_a were undertaken to determine whether optimal properties could be found within this basic series. Modification of the pyrrolidine

Table 2. SAR of Weakly Basic Amines



compound	R	hDGAT2 IC ₅₀ (nM) ^a	pK _a ^b	logD ^c	HHEP CL _{int,app} (μL/min/million) ^d	P _{app} (10 ⁻⁶ cm/sec) ^e
6 ^f		4.4 (2.4 – 8.2)	4.5	2.8	38	30
7 ^g		140 (120 – 160)	5.2	2.3	9.3	14
8 ^h		480 (190 – 1,200)	6.4	1.8	4.7	18
9		16 (8.8 – 28)	8.0	0.96	<1.9	4.7
10		110 (59 – 220)	7.3	1.4	<1.9	8.8
11		200 (55 – 720)	6.8	1.7	6.6	13
12		10 (7.6 – 14)	7.5	1.4	0.99 ⁱ	2.9
13		42 (12 – 140)	7.5	1.3	<1.9	2.5

^aIC₅₀ values are reported as the geometric mean of $n \geq 3$ with the 95% CI in parentheses, except where otherwise noted. ^bExperimental pK_a. ^cExperimental logD using the shake-flask method at pH 7.4. ^dApparent intrinsic clearance (CL_{int,app}) obtained from human hepatocyte cells. ^ePermeability determined from an assay using low-efflux MDCKII cells. ^f6 is the more potent *cis* enantiomer; stereochemistry arbitrarily assigned. ^g7 is the more potent enantiomer; stereochemistry arbitrarily assigned. ^h8 is the more potent enantiomer; stereochemistry arbitrarily assigned. ⁱCL_{int,app} obtained from human hepatocyte cells using the relay method for low-clearance compounds.³⁷

and piperidine motifs was straightforward using readily available substituted building blocks. While the unsubstituted pyrrolidines were more potent than the corresponding piperidines, the greatest optimization potential was found with 3-aminopiperidines. Optimization of the piperidine motif with fluorine substitution is shown in Table 2. Fluorine substitution is known to alter the pK_a of a nearby nitrogen atom and can offer the advantage of improving permeability and metabolic stability in certain cases.²⁵

The addition of an α -trifluoromethyl group (6) lowered the pK_a by ~ 5 units and raised the logD by ~ 2.5 units compared to unsubstituted comparators 4 and 5. A significant improvement in DGAT2 potency was observed, along with increased permeability. Unfortunately, human hepatocyte clearance was markedly increased. Difluorination of the β -position (7) relative to the basic center increased the pK_a, and γ -

difluorination (8) increased the pK_a further, relative to 6. These analogues showed relatively lower lipophilicity, permeability, and clearance, with each of these properties trending with basicity.

To further improve potency and reduce clearance, monofluoro substitution was also examined. Compounds 9 and 10 include isomers with γ -substitution. These inhibitors showed the expected higher pK_a and lower lipophilicity relative to the difluoro version. Biochemical potency was improved, especially for 9, and both isomers showed lower clearance and good permeability. Examining the β -substituted monofluoro isomers (11–13), the basicity was moderately reduced and the lipophilicity was moderately increased, on average, as expected compared to the more distal γ -fluorinated analogues 9 and 10. There are also notable differences in basicity between β -substituted monofluoro isomers. Presumed axially substituted

Table 3. In Vivo Pharmacokinetic Profile in Preclinical Species^a

compound	species	CL (mL min ⁻¹ kg ⁻¹)	CL _r (mL min ⁻¹ kg ⁻¹)	V _{ss} (L/kg)	t _{1/2} i.v./p.o. (h)	F (%)
ervogastat	rat	61	<0.1	0.91	0.3/1.4 ^e	31
ervogastat	monkey ^b	10	<0.1	0.71	1.0/3.9	48
2	rat	51	5.2	4.1	1.9/NR	<1
12	rat ^c	64	7.5	2.7	0.9/NR	12 ^f
12	monkey ^d	17	0.29	1.6	1.4/6.5	21
12	dog	22	5.5	2.1	1.5/ND	ND

^aPharmacokinetic parameters were calculated from plasma concentration–time data and are reported as mean values. Intravenous (iv) PK (1 mg/kg) was conducted in male sex of each species (Wistar Han rats, beagle dogs and cynomolgus monkey, $n = 2$, except where otherwise noted). Solution formulation for the iv dose included 10% dimethyl sulfoxide (DMSO)/30% poly(ethylene glycol) (PEG) 400/60% water for rat and 23% hydroxypropyl- β -cyclodextrin (HPBCD) in water in dog and monkey except where noted. Oral (po) studies were administered as suspensions in 0.5% methylcellulose, except where noted. F was calculated using $AUC_{0-\infty}$, except where noted. NR = not reported due to insufficient regression points. ND = not determined. ^bSolution formulation for iv monkey study included 2% dimethylacetamide/98% (20% sulfobutylether- β -cyclodextrin (SBECD) in water). ^cSolution formulation for po rat study included 0.5% methylcellulose. ^dOral (po) study administered as a solution in 23% w/v HPBCD in water. ^e $n = 5$. ^f $AUC_{0-t_{last}}$ was used since regression points were not selected.

fluorine enantiomers **12** and **13** are more basic than the presumed equatorial racemic mixture of **11**. This has also been observed previously^{25–30} and is likely due to the antiparallel dipole interaction that stabilizes the protonated form in only the axial case. It is noticeable that metabolic clearance and permeability showed some correlation with the observed pK_a of the piperidine, with markedly higher values for both parameters as pK_a moved below physiological values. However, the correlation of potency with pK_a was much less clear, suggesting more subtle influences of specific fluorine placement. The *S,S* isomer, **12**, also showed excellent potency (>300-fold improvement relative to **2**), displayed very low hepatocyte clearance, and had acceptable permeability. This isomer was selected for further characterization.

Potency was also assessed in cryopreserved human hepatocytes by measuring [¹⁴C]glycerol incorporation into triglycerides using thin-layer chromatography. A selective DGAT1 inhibitor was added to this cellular assay to enhance the window to observe DGAT2-mediated triglyceride synthesis. In this assay, **12** showed an IC_{50} (95% CI) of 11 nM (8.6–15 nM). Compound **9** was somewhat less potent in the cryopreserved human hepatocyte assay with an IC_{50} (95% CI) of 23 nM (19–28 nM), strengthening the decision to pursue **12**. Selectivity was demonstrated by testing **12** against related acyltransferases (DGAT1, MGAT1, MGAT2, and MGAT3: all $IC_{50} > 50,000$ nM) and a broad off-target panel (Table S1).

Table 3 shows the pharmacokinetic parameters observed in both rat and monkey after iv administration of both **12** and ervogastat as a comparison. The observed volume of distribution of weakly basic **12** is 2- to 3-fold higher than that observed for neutral ervogastat in both rat and monkey. In addition, since the clearance appears comparable across compounds, this leads to a longer half-life for **12** in the species examined: 0.9 h in rat and 1.4 h in monkey. The bioavailability of **12** is 2- to 3-fold lower in rat and monkey compared to ervogastat, likely due to the lower in vitro passive permeability of **12**.

In keeping with the Extended Clearance Classification System (ECCS)³¹ class 4 designation of **12**, hepatic metabolism and renal clearance are predicted to be major clearance mechanisms. Preliminary human clearance for **12** was estimated by scaling the in vitro $CL_{int,app}$ in human hepatocytes (Table 2) using the well-stirred model. Renal clearance in humans was estimated using simple allometry from rat and dog.³² The human volume of distribution of **12**

was estimated to be moderate (2.3 L/kg) utilizing the Rogers and Rowland³³ tissue K_p calculation with predicted preclinical V_{ss} being within 2-fold of the observed value using the same method. Single-species scaling across preclinical species predicted a moderate V_{ss} (1.5–2.4 L/kg). In comparison, for ervogastat, the Rogers and Rowland tissue K_p calculation predicted a V_{ss} of 1.2 L/kg, and single-species scaling predicted a low to moderate V_{ss} (0.7–1.5 L/kg). For **12**, along with adequate oral absorption, a projected human half-life of approximately 8 h was considered acceptably longer than ervogastat to progress to further preclinical characterization.

Compound **12** was next examined for metabolic effects in vivo. The rat DGAT2 in vitro potency was similar to that of human (rat DGAT2 IC_{50} (95% CI) = 17 nM (9.1–33 nM)). Rats placed on a high-fat, high-sucrose, high cholesterol (Western) diet were treated orally twice daily for 8 days with **12**. An observed dose-dependent reduction in plasma and liver triglycerides resulted, as shown in Figure 2, with the high dose achieving a 71% reduction in plasma triglycerides and 48% reduction in liver triglycerides. While plasma triglycerides returned to chow-vehicle control levels at the top doses, a partial reduction was observed for hepatic triglycerides, similar to results observed with ervogastat in this same assay.¹² The partial reduction of hepatic triglycerides could be due to the inhibition of lipoprotein secretion from blunted hepatic SREBP signaling, a known regulator of lipoprotein secretion that we have demonstrated to be suppressed with DGAT2 inhibition.¹⁶ Compound **12** also reduced multiple SREBP target genes (Table S2), which also contributes to reduced de novo lipogenesis. Dose-dependent reductions in hepatic and circulating triglycerides, along with SREBP target gene expression reduction, were also noted after single-dose administration to high-sucrose-diet-fed rats (Figures S2 and S1 and Tables S4 and S3).

Adding a basic center in this case was a successful strategy to identify a DGAT2 inhibitor with an extended preclinical and predicted human half-life. A balanced basicity and lipophilicity profile was needed to achieve an acceptable suite of attributes, including potency, permeability, and clearance. Ultimately an ideal balance of basicity and lipophilicity was achieved through the strategic introduction of fluorine to the piperidine ring, to arrive at monofluorinated derivative **12**. This molecule, PF-07202954, was nominated as a development candidate and advanced to phase I clinical trials in order to determine its human pharmacokinetic profile.

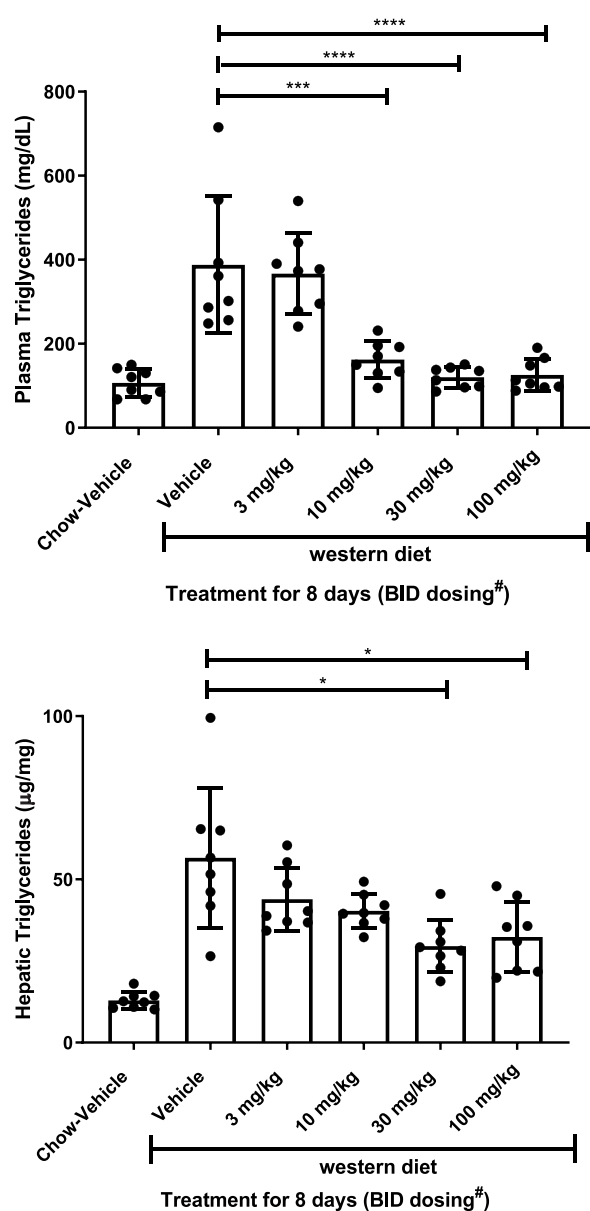


Figure 2. Plasma and hepatic triglycerides in Western-diet-fed rats after an 8-day treatment with 12. Data are mean \pm standard deviation from eight animals per group. The difference between group means relative to the Western diet vehicle was performed by one-way ANOVA taking account for unequal variance followed by a Dunnett's multiple comparisons test. ****, $p < 0.0001$ relative to Western diet vehicle-treated animals; ***, $p < 0.001$ relative to Western diet vehicle-treated animals; *, $p < 0.05$ relative to Western diet vehicle-treated animals. BID dose administration was separated by 8 h. #On day 8 a single dose was administered in the morning, and animals were sacrificed 2 h after treatment.

ASSOCIATED CONTENT

Supporting Information

The Supporting Information is available free of charge at <https://pubs.acs.org/doi/10.1021/acsmchemlett.3c00330>.

Synthetic procedures and characterization data for analogues 1–13, activity in a broad off-target panel, in vitro and hepatocyte assay procedures, in vivo protocols and results for 8-day treatment of Western-diet-fed rats and single-dose treatment of sucrose-diet-fed rats, both with PF-07202954 (12) (PDF)

AUTHOR INFORMATION

Corresponding Author

Kevin J. Filipksi – Pfizer Research & Development, Cambridge, Massachusetts 02139, United States; orcid.org/0000-0003-0845-5723; Email: kevin.filipksi@pfizer.com

Authors

David J. Edmonds – Pfizer Research & Development, Cambridge, Massachusetts 02139, United States; orcid.org/0000-0001-9234-8618
 Michelle R. Garnsey – Pfizer Research & Development, Cambridge, Massachusetts 02139, United States; Pfizer Research & Development, Groton, Connecticut 06340, United States; orcid.org/0000-0003-1226-1868
 Daniel J. Smaltz – Pfizer Research & Development, Cambridge, Massachusetts 02139, United States; Pfizer Research & Development, Groton, Connecticut 06340, United States
 Karen Coffman – Pfizer Research & Development, Groton, Connecticut 06340, United States
 Kentaro Futatsugi – Pfizer Research & Development, Cambridge, Massachusetts 02139, United States
 Jack Lee – Pfizer Research & Development, Groton, Connecticut 06340, United States; orcid.org/0000-0003-0477-8568
 Steven V. O'Neil – Pfizer Research & Development, Groton, Connecticut 06340, United States
 Ann Wright – Pfizer Research & Development, Groton, Connecticut 06340, United States
 Deane Nason – Pfizer Research & Development, Groton, Connecticut 06340, United States
 James R. Gosset – Pfizer Research & Development, Cambridge, Massachusetts 02139, United States
 Christine C. Orozco – Pfizer Research & Development, Groton, Connecticut 06340, United States; orcid.org/0009-0001-4971-5491
 Dan Blackler – Pfizer Research & Development, Cambridge, Massachusetts 02139, United States
 Guila Fakhoury – Pfizer Research & Development, Cambridge, Massachusetts 02139, United States
 Jemy A. Gutierrez – Pfizer Research & Development, Cambridge, Massachusetts 02139, United States
 Sylvie Perez – Pfizer Research & Development, Cambridge, Massachusetts 02139, United States
 Trenton Ross – Pfizer Research & Development, Cambridge, Massachusetts 02139, United States
 Ingrid Stock – Pfizer Research & Development, Groton, Connecticut 06340, United States
 Gregory Tesz – Pfizer Research & Development, Cambridge, Massachusetts 02139, United States
 Robert Dullea – Pfizer Research & Development, Cambridge, Massachusetts 02139, United States

Complete contact information is available at: <https://pubs.acs.org/doi/10.1021/acsmchemlett.3c00330>

Author Contributions

The manuscript was written through contributions of all authors. All of the authors approved the final version of the manuscript.

Notes

All experiments involving animals were conducted in our AAALAC-accredited facilities and were reviewed and approved by Pfizer Institutional Animal Care and Use Committee (IACUC).

The authors declare the following competing financial interest(s): All authors were employees of Pfizer, Inc. at the time that work was done and may own Pfizer stock. This work was financially supported by Pfizer, Inc.

ACKNOWLEDGMENTS

We thank Junshan Luo, Juan Shi, and Wenjuan Wong at Wuxi AppTec as well as Kim Huard and Esther Lee for their contributions.

ABBREVIATIONS

NAFLD, non-alcoholic fatty liver disease; NASH, non-alcoholic steatohepatitis; DGAT2, diacylglycerol O-acyltransferase 2; DGAT1, diacylglycerol O-acyltransferase 1; $t_{1/2}$, half-life; V_{ss} , steady-state volume of distribution; ECCS, Extended Clearance Classification System; D , distribution; HHEP, human hepatocyte; P_{app} , apparent permeability; CL, clearance; SREBP, sterol regulatory element-binding protein

REFERENCES

(1) Fon Tacer, K.; Rozman, D. Nonalcoholic Fatty liver disease: focus on lipoprotein and lipid deregulation. *J. Lipids* **2011**, *2011*, 783976.

(2) Haas, J. T.; Francque, S.; Staels, B. Pathophysiology and Mechanisms of Nonalcoholic Fatty Liver Disease. *Annu. Rev. Physiol.* **2016**, *78*, 181–205.

(3) Yen, C. L.; Stone, S. J.; Koliwad, S.; Harris, C.; Farese, R. V. Jr. Thematic review series: glycerolipids. DGAT enzymes and triacylglycerol biosynthesis. *J. Lipid Res.* **2008**, *49* (11), 2283–2301.

(4) Amin, N. B.; Saxena, A. R.; Somayaji, V.; Dullea, R. Inhibition of Diacylglycerol Acyltransferase 2 Versus Diacylglycerol Acyltransferase 1: Potential Therapeutic Implications of Pharmacology. *Clin. Ther.* **2023**, *45* (1), 55–70.

(5) Choi, S. H.; Ginsberg, H. N. Increased very low density lipoprotein (VLDL) secretion, hepatic steatosis, and insulin resistance. *Trends Endocrinol. Metab.* **2011**, *22* (9), 353–363.

(6) Liu, Y.; Millar, J. S.; Cromley, D. A.; Graham, M.; Croke, R.; Billheimer, J. T.; Rader, D. J. Knockdown of acyl-CoA:diacylglycerol acyltransferase 2 with antisense oligonucleotide reduces VLDL TG and ApoB secretion in mice. *Biochim. Biophys. Acta* **2008**, *1781* (3), 97–104.

(7) Yu, X. X.; Murray, S. F.; Pandey, S. K.; Booten, S. L.; Bao, D.; Song, X. Z.; Kelly, S.; Chen, S.; McKay, R.; Monia, B. P.; Bhanot, S. Antisense oligonucleotide reduction of DGAT2 expression improves hepatic steatosis and hyperlipidemia in obese mice. *Hepatology* **2005**, *42* (2), 362–371.

(8) Vuppalanchi, R.; Nouredin, M.; Alkhoury, N.; Sanyal, A. J. Therapeutic pipeline in nonalcoholic steatohepatitis. *Nat. Rev. Gastroenterol. Hepatol.* **2021**, *18* (6), 373–392.

(9) Futatsugi, K.; Kung, D. W.; Orr, S. T.; Cabral, S.; Hepworth, D.; Aspnes, G.; Bader, S.; Bian, J.; Boehm, M.; Carpino, P. A.; Coffey, S. B.; Dowling, M. S.; Herr, M.; Jiao, W.; Lavergne, S. Y.; Li, Q.; Clark, R. W.; Erion, D. M.; Kou, K.; Lee, K.; Pabst, B. A.; Perez, S. M.; Purkal, J.; Jorgensen, C. C.; Goosen, T. C.; Gosset, J. R.; Niosi, M.; Pettersen, J. C.; Pfeifferkorn, J. A.; Ahn, K.; Goodwin, B. Discovery and optimization of imidazopyridine-based inhibitors of diacylglycerol acyltransferase 2 (DGAT2). *J. Med. Chem.* **2015**, *58* (18), 7173–7185.

(10) Futatsugi, K.; Huard, K.; Kung, D. W.; Pettersen, J. C.; Flynn, D. A.; Gosset, J. R.; Aspnes, G. E.; Barnes, R. J.; Cabral, S.; Dowling, M. S.; Fernando, D. P.; Goosen, T. C.; Gorczyca, W. P.; Hepworth,

D.; Herr, M.; Lavergne, S.; Li, Q.; Niosi, M.; Orr, S. T. M.; Pardo, I. D.; Perez, S. M.; Purkal, J.; Schmahaj, T. J.; Shirai, N.; Shoieb, A. M.; Zhou, J.; Goodwin, B. Small structural changes of the imidazopyridine diacylglycerol acyltransferase 2 (DGAT2) inhibitors produce an improved safety profile. *MedChemComm* **2017**, *8* (4), 771–779.

(11) McLaren, D. G.; Han, S.; Murphy, B. A.; Wilsie, L.; Stout, S. J.; Zhou, H.; Roddy, T. P.; Gorski, J. N.; Metzger, D. E.; Shin, M. K.; Reilly, D. F.; Zhou, H. H.; Tadin-Strapps, M.; Bartz, S. R.; Cumiskey, A. M.; Graham, T. H.; Shen, D. M.; Akinsanya, K. O.; Previs, S. F.; Imbriglio, J. E.; Pinto, S. DGAT2 inhibition alters aspects of triglyceride metabolism in rodents but not in non-human primates. *Cell Metab.* **2018**, *27* (6), 1236–1248.

(12) Futatsugi, K.; Cabral, S.; Kung, D. W.; Huard, K.; Lee, E.; Boehm, M.; Bauman, J.; Clark, R. W.; Coffey, S. B.; Crowley, C.; Dechert-Schmitt, A. M.; Dowling, M. S.; Dullea, R.; Gosset, J. R.; Kalgutkar, A. S.; Kou, K.; Li, Q.; Lian, Y.; Loria, P. M.; Londregan, A. T.; Niosi, M.; Orozco, C.; Pettersen, J. C.; Pfeifferkorn, J. A.; Polivkova, J.; Ross, T. T.; Sharma, R.; Stock, I. A.; Tesz, G.; Wisniewska, H.; Goodwin, B.; Price, D. A. Discovery of Ervogastat (PF-06865571): A Potent and Selective Inhibitor of Diacylglycerol Acyltransferase 2 for the Treatment of Non-alcoholic Steatohepatitis. *J. Med. Chem.* **2022**, *65* (22), 15000–15013.

(13) Imbriglio, J. E.; Shen, D. M.; Liang, R.; Marby, K.; You, M.; Youm, H. W.; Feng, Z.; London, C.; Xiong, Y.; Tata, J.; Verras, A.; Garcia-Calvo, M.; Song, X.; Addona, G. H.; McLaren, D. G.; He, T.; Murphy, B.; Metzger, D. E.; Salituro, G.; Deckman, D.; Chen, Q.; Jin, X.; Stout, S. J.; Wang, S. P.; Wilsie, L.; Palyha, O.; Han, S.; Hubbard, B. K.; Previs, S. F.; Pinto, S.; Taggart, A. Discovery and pharmacology of a novel class of diacylglycerol acyltransferase 2 inhibitors. *J. Med. Chem.* **2015**, *58* (23), 9345–9353.

(14) Camp, N. P.; Naik, M. Novel DGAT2 inhibitors. WO 2015077299, 2015.

(15) Escribano, A. M.; Gonzalez, M. R.; Lafuente Blanco, C.; Martin-Ortega Finger, M. D.; Wiley, M. R. Novel DGAT2 inhibitors. WO 2016187384, 2016.

(16) Amin, N. B.; Carvajal-Gonzalez, S.; Purkal, J.; Zhu, T.; Crowley, C.; Perez, S.; Chidsey, K.; Kim, A. M.; Goodwin, B. Targeting diacylglycerol acyltransferase 2 for the treatment of nonalcoholic steatohepatitis. *Sci. Transl. Med.* **2019**, *11* (520), No. eaav9701.

(17) Pfizer Product Pipeline. <https://www.pfizer.com/science/drug-product-pipeline> (accessed 2022-10-24).

(18) LG Chem Business Areas: Life Science. <https://www.lgchem.com/company/company-information/business-domain/biology> (accessed 2022-11-21).

(19) Loomba, R.; Morgan, E.; Watts, L.; Xia, S.; Hannan, L. A.; Geary, R. S.; Baker, B. F.; Bhanot, S. Novel antisense inhibition of diacylglycerol O-acyltransferase 2 for treatment of non-alcoholic fatty liver disease: a multicentre, double-blind, randomised, placebo-controlled phase 2 trial. *Lancet Gastroenterol. Hepatol.* **2020**, *5* (9), 829–838.

(20) Ionis Pipeline. <https://www.ionispharma.com/ionis-innovation/pipeline/> (accessed 2022-10-31).

(21) Smith, D. A.; Beaumont, K.; Maurer, T. S.; Di, L. Relevance of half-life in drug design. *J. Med. Chem.* **2018**, *61* (10), 4273–4282.

(22) Gunaydin, H.; Altman, M. D.; Ellis, J. M.; Fuller, P.; Johnson, S. A.; Lahue, B.; Lapointe, B. Strategy for extending half-life in drug design and its significance. *ACS Med. Chem. Lett.* **2018**, *9* (6), 528–533.

(23) Smith, D. A.; Beaumont, K.; Maurer, T. S.; Di, L. Volume of distribution in drug design. *J. Med. Chem.* **2015**, *58* (15), 5691–5698.

(24) Edmonds, D. J.; Filipinski, K. J.; Futatsugi, K.; Garnsey, M. R.; Lee, J. C. H.; Smaltz, D. J. Preparation of piperidinyl pyrimidines as diacylglycerol acyltransferase 2 inhibitors. WO 2021064590, 2021.

(25) Gillis, E. P.; Eastman, K. J.; Hill, M. D.; Donnelly, D. J.; Meanwell, N. A. Applications of fluorine in medicinal chemistry. *J. Med. Chem.* **2015**, *58* (21), 8315–8359.

(26) van Niel, M. B.; Collins, I.; Beer, M. S.; Broughton, H. B.; Cheng, S. K.; Goodacre, S. C.; Heald, A.; Locker, K. L.; MacLeod, A. M.; Morrison, D.; Moyes, C. R.; O'Connor, D.; Pike, A.; Rowley, M.;

Russell, M. G.; Sohal, B.; Stanton, J. A.; Thomas, S.; Verrier, H.; Watt, A. P.; Castro, J. L. Fluorination of 3-(3-(piperidin-1-yl)propyl)indoles and 3-(3-(piperazin-1-yl)propyl)indoles gives selective human 5-HT_{1D} receptor ligands with improved pharmacokinetic profiles. *J. Med. Chem.* **1999**, *42* (12), 2087–2104.

(27) Cox, C. D.; Coleman, P. J.; Breslin, M. J.; Whitman, D. B.; Garbaccio, R. M.; Fraley, M. E.; Buser, C. A.; Walsh, E. S.; Hamilton, K.; Schaber, M. D.; Lobell, R. B.; Tao, W.; Davide, J. P.; Diehl, R. E.; Abrams, M. T.; South, V. J.; Huber, H. E.; Torrent, M.; Prueksaritanont, T.; Li, C.; Slaughter, D. E.; Mahan, E.; Fernandez-Metzler, C.; Yan, Y.; Kuo, L. C.; Kohl, N. E.; Hartman, G. D. Kinesin spindle protein (KSP) inhibitors. 9. Discovery of (2*S*)-4-(2,5-difluorophenyl)-*N*-[(3*R*,4*S*)-3-fluoro-1-methylpiperidin-4-yl]-2-(hydroxymethyl)-*N*-methyl-2-phenyl-2,5-dihydro-1*H*-pyrrole-1-carboxamide (MK-0731) for the treatment of taxane-refractory cancer. *J. Med. Chem.* **2008**, *51* (14), 4239–4252.

(28) Nairoukh, Z.; Strieth-Kalthoff, F.; Bergander, K.; Glorius, F. Understanding the conformational behavior of fluorinated piperidines: the origin of the axial-F preference. *Chem. - Eur. J.* **2020**, *26* (28), 6141–6146.

(29) Nairoukh, Z.; Strieth-Kalthoff, F.; Bergander, K.; Glorius, F. Corrigendum: Understanding the conformational behavior of fluorinated piperidines: the origin of the axial-F preference. *Chem. - Eur. J.* **2020**, *26* (61), 14018–14019.

(30) Morgenthaler, M.; Schweizer, E.; Hoffmann-Roder, A.; Benini, F.; Martin, R. E.; Jaeschke, G.; Wagner, B.; Fischer, H.; Bendels, S.; Zimmerli, D.; Schneider, J.; Diederich, F.; Kansy, M.; Muller, K. Predicting and tuning physicochemical properties in lead optimization: amine basicities. *ChemMedChem* **2007**, *2* (8), 1100–1115.

(31) Varma, M. V.; Steyn, S. J.; Allerton, C.; El-Kattan, A. F. Predicting clearance mechanism in drug discovery: Extended Clearance Classification System (ECCS). *Pharm. Res.* **2015**, *32* (12), 3785–3802.

(32) Paine, S. W.; Menochet, K.; Denton, R.; McGinnity, D. F.; Riley, R. J. Prediction of human renal clearance from preclinical species for a diverse set of drugs that exhibit both active secretion and net reabsorption. *Drug Metab. Dispos.* **2011**, *39* (6), 1008–1013.

(33) Rodgers, T.; Leahy, D.; Rowland, M. Physiologically based pharmacokinetic modeling 1: predicting the tissue distribution of moderate-to-strong bases. *J. Pharm. Sci.* **2005**, *94* (6), 1259–1276.

(34) Stopher, D.; McClean, S. An improved method for the determination of distribution coefficients. *J. Pharm. Pharmacol.* **1990**, *42* (2), 144.

(35) Keefer, C.; Chang, G.; Carlo, A.; Novak, J. J.; Banker, M.; Carey, J.; Cianfrogna, J.; Eng, H.; Jagla, C.; Johnson, N.; Jones, R.; Jordan, S.; Lazzaro, S.; Liu, J.; Scott Obach, R.; Riccardi, K.; Tess, D.; Umland, J.; Racich, J.; Varma, M.; Visswanathan, R.; Di, L. Mechanistic insights on clearance and inhibition discordance between liver microsomes and hepatocytes when clearance in liver microsomes is higher than in hepatocytes. *Eur. J. Pharm. Sci.* **2020**, *155*, 105541.

(36) Di, L.; Whitney-Pickett, C.; Umland, J. P.; Zhang, H.; Zhang, X.; Gebhard, D. F.; Lai, Y.; Federico, J. J., 3rd; Davidson, R. E.; Smith, R.; Reyner, E. L.; Lee, C.; Feng, B.; Rotter, C.; Varma, M. V.; Kempshall, S.; Fenner, K.; El-Kattan, A. F.; Liston, T. E.; Troutman, M. D. Development of a new permeability assay using low-efflux MDCKII cells. *J. Pharm. Sci.* **2011**, *100* (11), 4974–4985.

(37) Di, L.; Trapa, P.; Obach, R. S.; Atkinson, K.; Bi, Y. A.; Wolford, A. C.; Tan, B.; McDonald, T. S.; Lai, Y.; Tremaine, L. M. A novel relay method for determining low-clearance values. *Drug Metab. Dispos.* **2012**, *40* (9), 1860–1865.